risks

MDPI

Article

Adding Shocks to a Prospective Mortality Model

Frédéric Planchet [1,2,*] and Guillaume Gautier de La Plaine [1]

[1] Prim'Act, 75017 Paris, France; guillaume.gautierdelaplaine@primact.fr
[2] ISFA, Institut de Science Financière et d'Assurances (ISFA), Laboratoire SAF EA2429, Université de Lyon, Université Claude Bernard Lyon 1, 69366 Lyon, France
* Correspondence: frederic@planchet.net

Abstract: This work proposes a simple model to take into account the annual volatility of the mortality level observed on the scale of a country like France in the construction of prospective mortality tables. By assigning a frailty factor to a basic hazard function, we generalise the Lee–Carter model. The impact on prospective life expectancies and capital requirements in the context of a life annuity scheme is analysed in detail.

Keywords: longevity risk; prospective mortality tables

check for updates

Citation: Planchet, Frédéric, and Guillaume Gautier de La Plaine. 2024. Adding Shocks to a Prospective Mortality Model. *Risks* 12: 57. https://doi.org/10.3390/risks12030057

Academic Editor: Han Li

Received: 2 January 2024
Revised: 12 March 2024
Accepted: 15 March 2024
Published: 20 March 2024

1. Introduction

The construction of life expectancy projections has been the subject of many works since the seminal article by Lee and Carter (Lee and Carter 1992).

For the purpose of extrapolating trends observed in the past into the future, most of the approaches that have been proposed are based on a "mortality surface", which measures mortality forces by age and year at a given time, and smoothly extrapolates these into the future.

The models inspired by Lee and Carter start by reducing dimensions by performing a PCA and then extrapolating one or two time series associated with the projection on the principal axes (see Plat 2009 for a detailed discussion).

Bongaarts (Bongaarts 2004) proposed a different approach, based on parametric adjustments by year of time vs. year of age and extrapolation of the estimated coefficients each year.

In Bongaarts (2004), however, the author uses a rather simple parametric representation (Thatcher's model, see Thatcher 1999), which does not allow all ages to be included. Moreover, he limits his extrapolation to two out of three parameters (the age structure of the mortality is assumed to be independent of time), treating them independently, which is a questionable approximation (time varying coefficients for accident and aging should be dependent).

This type of model projects a smooth $t \to \mu(x,t)$ series. Given $\mu(x,t)$ and the risk exposures $E(x,t)$, we compute the annual global mortality rate in France, $q(t) = \sum_x E(x,t) \times \mu(x,t) / \sum_x E(x,t)$. When looking at annual variations in this mortality rate from 1982 to 2022 (see Figure 1), we see a rather high degree of volatility. On this figure, the red line is the annual variation of mortality, whereas the blue line is a quadratic fit of this annual variation.

The classic models described above cannot easily account for these short-term variations. The "probabilistic version" of the Lee–Carter model proposed by Brouhns et al. (2002) could be used as a stochastic mortality model, but at the cost of being somewhat cumbersome to implement. What is more, the uncertainty included in this model refers solely to the estimation risk, whereas here we are seeking to account for a different kind of uncertainty, relating to the underlying mortality itself. Proposed approaches for this have been put forward, for example, in Guette (2010) or Currie et al. (2003), but with

a slightly different objective, as these works propose to model catastrophes (rare high-intensity events) such as wars or severe epidemics. More recently, an approach using regime-switching models was proposed in Robben and Antonio (2023).

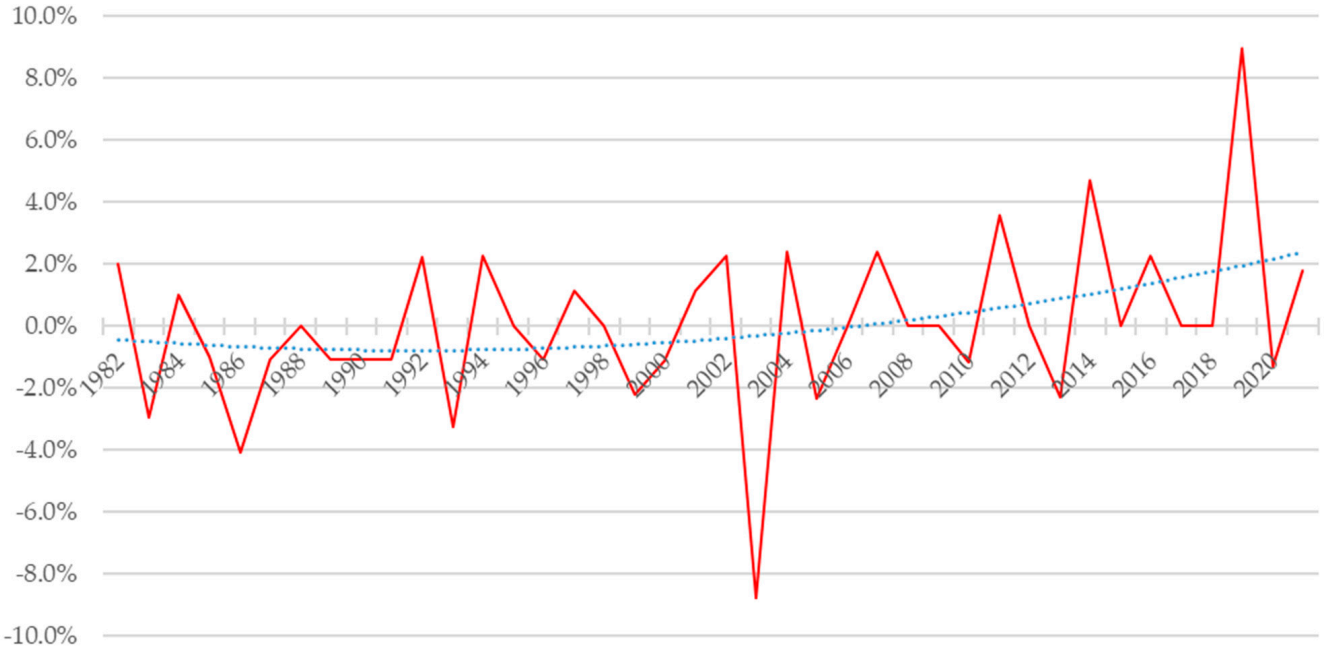

Figure 1. Annual variation in global mortality rate in France (1982 to 2022).

However, our aim here is not to model rare events, but to incorporate the above volatility into the model, in order to provide a more accurate assessment of residual life expectancies when an unbiased estimate of mortality rates is available. We are not concerned here with trend risk, for which there are many models (see Juillard et al. 2008; Juillard and Planchet 2006; Plat 2009), but only with the short-term shift in mortality trend.

Therefore, a specific approach is proposed here, with the aim of accounting for this short-term volatility and measuring its impact on the anticipation of prospective residual life expectancies in a parsimonious way.

We draw inspiration here from the frailty models proposed by Vaupel and his co-authors (Vaupel et al. 1979) by applying to a regular base hazard function a shock that depends only on time, under a proportional hazards assumption. This model was generalised by Barbi (1999), who proposed a heterogeneity model called "combined fragility", still assuming proportional fragility initially distributed according to a Gamma distribution. It is used in Barbi et al. (2003), for example, to study the extreme age of survival.

Very recently, Carannante et al. (2023) offered a frailty version of the Lee–Carter model which is very close to ours.

The frailty factor is not used here to consider population heterogeneity, as is usually the case, but to introduce uncertainty into the model's basic hazard function. The frailty factor is thus designed to account for annual shifts around a steady mortality trend.

For further references, reader may look at (Debonneuil 2015; Guilbaud 2018; Planchet and Thérond 2011).

2. Proposed Stochastic Mortality Model

The proposed specification is described below, followed by a method for estimating the parameters within the framework of conditional maximum likelihood.

2.1. Specification

Consider the following specification of the (stochastic) hazard function for the year of time *t:*

$$\mu(x,t) = Z_t \times \mu_0(x,t) \tag{1}$$

with the semi-parametric form of the basic hazard function $ln\mu_0(x,t) = \alpha_x + \beta_x k_t$. The shocks at time t are introduced through the random variable Z_t. These shocks are assumed to be independent, identically distributed and mean-centred, i.e., $E(Z_t) = 1$. Because k_t is assumed to be deterministic, this model differs from the one described in Plat (2009). What is more, in his article, Plat proposes interesting ways to model uncertainty about the mortality trend. Here, we are interested in short-term deviations in the level of mortality, with all ages combined. The two approaches are, therefore, complementary and do not consider the same risks.

We use the usual identifiability conditions for the basic hazard function, which are imposed[1] as follows (cf. Brouhns et al. 2002):

$$\sum_{x=x_m}^{x_M} \beta_x = 1 \tag{2}$$

and

$$\sum_{t=t_m}^{t_M} k_t = 0 \tag{3}$$

This involves estimating the parameters of Z_t and the matrix (α, β, k), then extrapolating the time series $t \to k_t$.

2.2. Log-Likelihood Determination

For maximum likelihood estimation, we know that everything happens as if the number of deaths observed followed a Poisson distribution,

$$D_{x,t} \sim P(E_{x,t} \times \mu(x,t)), \tag{4}$$

which leads to the following expression for the conditional likelihood for an observation, noting $\lambda = E_{x,t} \times \mu_0(x,t)$ and $Z = Z_t$:

$$P(D = d|Z) = e^{-\lambda Z} \frac{\lambda^d}{d!} Z^d. \tag{5}$$

Likelihood for one observation is easy to obtain:

$$P(D = d) = E_Z[P(D = d|Z)] = \int e^{-\lambda z} z^d \frac{\lambda^d}{d!} dF_Z(z). \tag{6}$$

We then choose a Gamma distribution of parameters a and b for the distribution of Z_t, i.e., $f_Z(z) = z^{a-1} \frac{b^a e^{-b \times z}}{\Gamma(a)}$, which leads to

$$P(D = d) = \frac{\lambda^d}{d!} \frac{b^a}{\Gamma(a)} \int_0^{+\infty} e^{-(\lambda+b)z} z^{d+a-1} dz. \tag{7}$$

Using the change of variable $u = (\lambda + b)z$, we obtain the following expression for the likelihood of an observation

$$P(D = d) = \frac{\lambda^d}{d!} \frac{b^a}{\Gamma(a)} \frac{1}{(\lambda+b)^{d+a}} \int_0^{+\infty} e^{-u} u^{d+a-1} du, \tag{8}$$

which gives

$$P(D = d) = \frac{\lambda^d}{d!}\frac{b^a}{\Gamma(a)}\frac{1}{(\lambda + b)^{d+a}}\Gamma(d + a), \tag{9}$$

which in turn gives log-likelihood

$$lnP(D = d) = f(a, b) + dln(\lambda) - (d + a)ln(\lambda + b), \tag{10}$$

with $f(a, b) = ln\left(b^a \frac{\Gamma(d+a)}{\Gamma(d+1)\Gamma(a)}\right)$.

As a function of the parameters (α, β, k) and conditional on (a, b), the log-likelihood for an observation is of the form $l(\alpha, \beta, k) = lnP(D = d)$ with $\lambda = E_{x,t} \times \mu_0(x, t) = E_{x,t} \times e^{\alpha_x + \beta_x k_t}$. Conditional on (a, b), the log-likelihood has the following form (with one additive constant):

$$lnL = \sum_{x=x_m}^{x_M} \sum_{t=t_m}^{t_M} lnP(D_{x,t} = d_{x,t}|a, b), \tag{11}$$

which gives

$$lnL = \sum_{x=x_m}^{x_M} \sum_{t=t_m}^{t_M} [d_{x,t} ln(\lambda_{x,t}) - (d_{x,t} + a)ln(\lambda_{x,t} + b)]. \tag{12}$$

Ultimately, this model aims to study the extent to which short-term volatility of mortality rates may impact prospective mortality rates. It is accomplished through the presence of parameters a and b in the log-likelihood, which can then be maximised by (α, β, k) under the constraint given by Equations (2) and (3). This task is performed in the next section.

2.3. Parameter Estimation

Parameter estimation can be carried out in two stages: in the first stage, the frailty parameter is estimated, then, in the second stage, the above log-likelihood is maximised at (α, β, k).

The condition $E(Z_t) = 1$ implies $a = b$. We also have $V(Z_t) = \frac{a}{b^2} = \frac{1}{a}$, so the disturbance control parameter Z_t is the inverse of the variance $a = \sigma_Z^{-2}$. A direct estimate of this parameter can be made as follows, observing that the mean annual output intensities are of the form

$$\overline{\mu}(t) = Z_t \times \overline{\mu}_0(t), \tag{13}$$

with

$$\overline{\mu}_0(t) = \frac{\sum_{x=x_m}^{x_M} E_{x,t}\mu_0(x, t)}{\sum_{x=x_m}^{x_M} E_{x,t}}, \tag{14}$$

from which we derive $E(\overline{\mu}(t)) = \overline{\mu}_0(t)$, $V(\overline{\mu}(t)) = V(Z_t)\overline{\mu}_0^2(t)$ then $V(Z_t) = \frac{V(\overline{\mu}(t))}{E(\overline{\mu}(t))^2}$. That last equation is equivalent to $\sigma(Z_t) = cv(\overline{\mu}(t))$, with $cv(\overline{\mu}(t))$ being the coefficient of variation of $\overline{\mu}(t)$ and $\sigma(Z_t)$ being the standard deviation of Z_t.

It is then straightforward to use the usual estimator for $V(Z_t)$:

$$\hat{\sigma}_Z^2 = \frac{\frac{1}{t_M - t_m + 1}\sum_{t=t_m}^{t_M}\left(\hat{\mu}(t) - \frac{1}{t_M - t_m + 1}\sum_{t=t_m}^{t_M}\hat{\mu}(t)\right)^2}{\left(\frac{1}{t_M - t_m + 1}\sum_{t=t_m}^{t_M}\hat{\mu}(t)\right)^2}. \tag{15}$$

with $\hat{\mu}(t)$ and $\hat{\mu}(x, t)$ corresponding to the Hoem estimator of the hazard function:

$$\hat{\mu}(t) = \frac{\sum_{x=x_m}^{x_M} E_{x,t}\hat{\mu}(x, t)}{\sum_{x=x_m}^{x_M} E_{x,t}}, \tag{16}$$

and

$$\hat{\mu}(x,t) = \frac{D_{x,t}}{E_{x,t}}. \tag{17}$$

Given that $a = \sigma_Z^{-2}$ and using Equation (15), the frailty parameter can be estimated as follows:

$$a = \frac{1}{\hat{\sigma}_Z^2} = \frac{\left(\frac{1}{t_M - t_m + 1}\sum_{t=t_m}^{t_M}\hat{\mu}(t)\right)^2}{\frac{1}{t_M - t_m + 1}\sum_{t=t_m}^{t_M}\left(\hat{\mu}(t) - \frac{1}{t_M - t_m + 1}\sum_{t=t_m}^{t_M}\hat{\mu}(t)\right)^2}. \tag{18}$$

Once the frailty parameter has been estimated, the aim is to maximise the previously expressed log-likelihood. The partial derivatives of the log-likelihood for an observation are as follows:

$$\frac{\partial}{\partial p} lnP(D = d) = d\frac{1}{\lambda}\frac{\partial \lambda}{\partial p} - (d + a)\frac{1}{\lambda + b}\frac{\partial \lambda}{\partial p} = \left(\frac{d}{\lambda} - \frac{d + a}{\lambda + a}\right)\frac{\partial \lambda}{\partial p}, \tag{19}$$

with p one of the parameters (α, β, k). Since

$$\frac{\partial \lambda}{\partial \alpha} = \lambda, \tag{20}$$

$$\frac{\partial \lambda}{\partial \beta} = k\lambda, \tag{21}$$

and

$$\frac{\partial \lambda}{\partial k} = \beta\lambda, \tag{22}$$

it is possible to estimate (α, β, k), as a solution of the following first-order conditions:

$$\frac{\partial}{\partial \alpha_x} lnL = \sum_{t=t_m}^{t_M}\left(\frac{d}{\lambda_{x,t}} - \frac{d + a}{\lambda_{x,t} + a}\right)\lambda_{x,t} = 0 \tag{23}$$

$$\frac{\partial}{\partial \beta_x} lnL = \sum_{t=t_m}^{t_M}\left(\frac{d}{\lambda_{x,t}} - \frac{d + a}{\lambda_{x,t} + a}\right)k_t\lambda_{x,t} = 0 \tag{24}$$

$$\frac{\partial}{\partial k_t} lnL = \sum_{x=x_m}^{x_M}\left(\frac{d}{\lambda_{x,t}} - \frac{d + a}{\lambda_{x,t} + a}\right)\beta_x\lambda_{x,t} = 0 \tag{25}$$

This system is non-linear.

2.4. Calculating Prospective Residual Life Expectancies

In the proposed model, the calculation of prospective life expectancy proceeds as follows

$$e(x,t) = E(e(x,t|Z)) = E\left(\sum_{i\geq 0}\prod_{j=0}^{i} exp\left(-\mu_{x+j,t+j}\right)\right) \tag{26}$$

Given the linearity of expectancy in a finite sum and knowing that the shocks are assumed to be independent, the prospective life expectancy takes the form

$$e(x,t) = \sum_{i\geq 0}\prod_{j=0}^{i} E\left(exp\left(-\mu_{x+j,t+j}\right)\right) \tag{27}$$

We then have

$$e(x,t) = \sum_{i\geq 0}\prod_{j=0}^{i}\left(\frac{a}{a + \mu_0(x + j, t + j)}\right)^a, \tag{28}$$

because the Laplace transform of a Gamma distribution is $E\left(e^{-xZ_t}\right) = \left(\frac{a}{a+x}\right)^a$. As $E\left(e^{-\mu(x,t)}\right) = E\left(e^{-Z_t \times \mu_0(x,t)}\right)$, we deduce that:

$$E\left(e^{-\mu(x,t)}\right) = E\left(e^{-Z_t \times \mu_0(x,t)}\right) = \left(\frac{a}{a+\mu_0(x,t)}\right)^a. \tag{29}$$

Note that $\lim_{a \to +\infty} E\left(e^{-\mu(x,t)}\right) = e^{-\mu_0(x,t)}$ and then we find the classic formula

$$e(x,t) = \sum_{i \geq 0} \prod_{j=0}^{i} exp(-\mu_0(x+j, t+j)). \tag{30}$$

3. Numerical Application

We use data for metropolitan France for the period of 2000 to 2020, with ages 0 to 105 included, from the Agalva and Blanpain (2021) study. The choice of these data is motivated by the desire to be consistent with the work of estimating future mortality of INSEE, which provided us with the data. The year 2020, which sees a significant increase in mortality compared to 2019 (which was, on the contrary, a year of particularly low mortality), is logically included in the study, as it is one of the non-catastrophic events (in the sense defined above) that we want to include in the modelling.

All calibration was performed in R 4.3.1.

Prospective analyses are then carried out over the entire age range and for the years of 2021 to 2060, to enable comparisons to prospective tables compiled by INSEE.

3.1. Model Adjustment

All of these steps are discussed in turn in the following subsections. Throughout the study, all of the results obtained are compared to those given by a Lee–Carter model calibrated on the same data.

3.1.1. Estimation of Gamma Distribution Parameters

The estimation of the pair of parameters (a, b) has been made with the raw data, and we find that $\sigma_Z^2 = 4.3\%$, i.e., $a = b = 550$.

3.1.2. Estimation of Model Parameters

The calibration of (α, β, k) under constraints was then carried out using the[2] Rsolnp package, and more specifically the solnp function (see Ghalanos and Theussl 2015). This function is based on the solver by Yinyu Ye (see Ye 1987).

In order to carry out this calibration, the results of a Lee–Carter model were chosen as initial parameters, calibrated using the lca function from the[3] demography package (see Hyndman 2023). All of these coefficients are transcribed in Appendix A.

As shown in the following figure (Figure 2), this leads to coefficients (α, β, k) that are very close to those of the referenced Lee–Carter model:

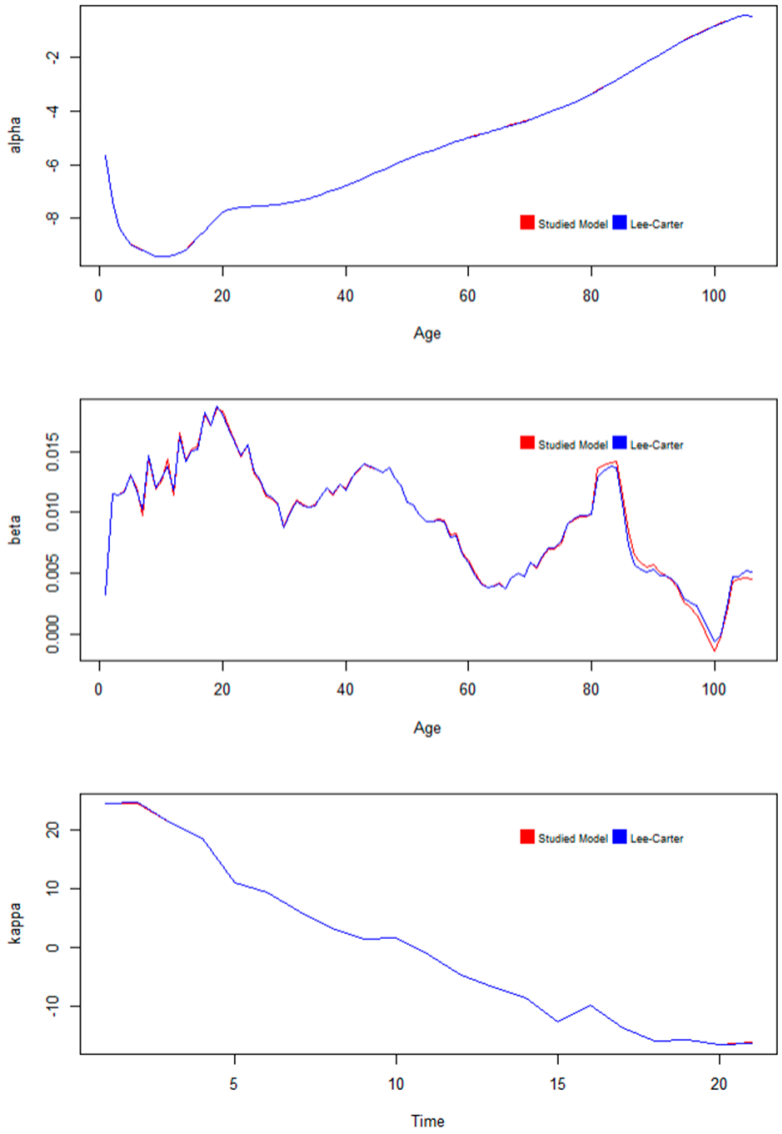

Figure 2. Comparison of the coefficients to those of a Lee–Carter model.

It can be seen that the time parameter shows a slower rate of decline from the 18th year of the observation period.

3.1.3. Extrapolation of Time Coefficients

Whether in the model studied here or in the Lee–Carter model used as a reference, the projection of coefficients $(k_t)_t$ for t beyond the calibration range have been performed by linear regression, by fitting the following equation to the calibrated parameters:

$$k_t = m \times t + p$$

In both cases, we find the coefficients shown in the following table (Table 1):

Table 1. Results of the extension of the time coefficients k.

	m	**p**
Model studied	−2.19	4401.98
Lee–Carter reference model	−2.19	4402.33

The results are logically very similar in both cases.

3.2. Projected Mortality Forces

Here, we compare projected mortality forces with and without shocks integrated into the model, as a function of age and year.

First, we look at the evolution of the mortality force as a function of age, for a few fixed years, as show in Figure 3:

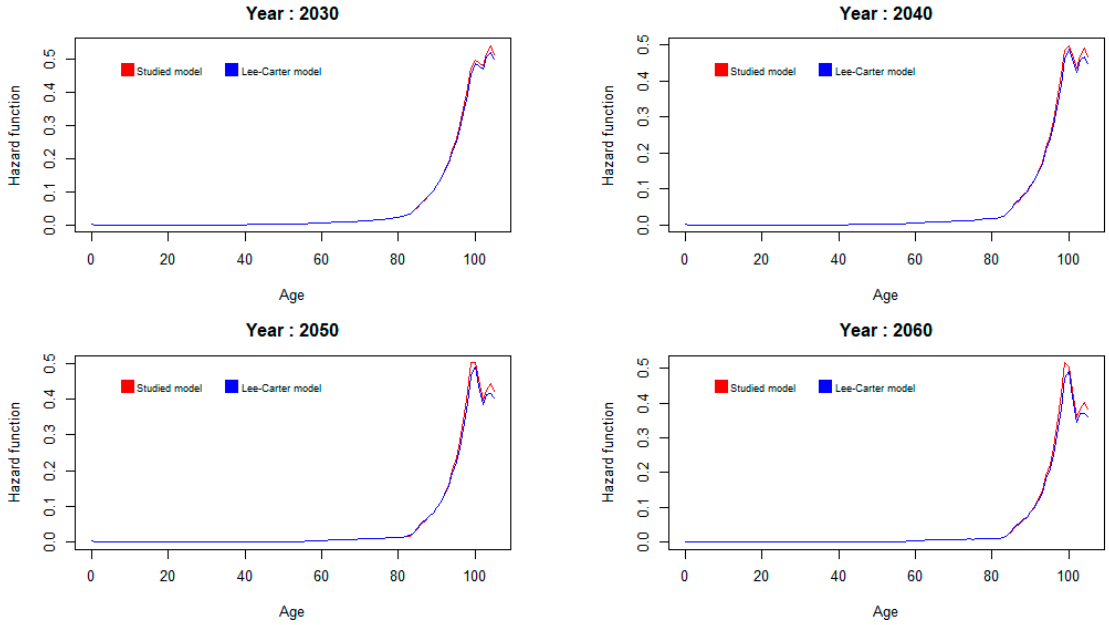

Figure 3. Mortality forces by age.

The mortality forces of the two models are very close, except at the highest ages, where the model with shocks tends to predict higher mortality forces. A closer look at the age range [90; 105] reveals the Figure 4:

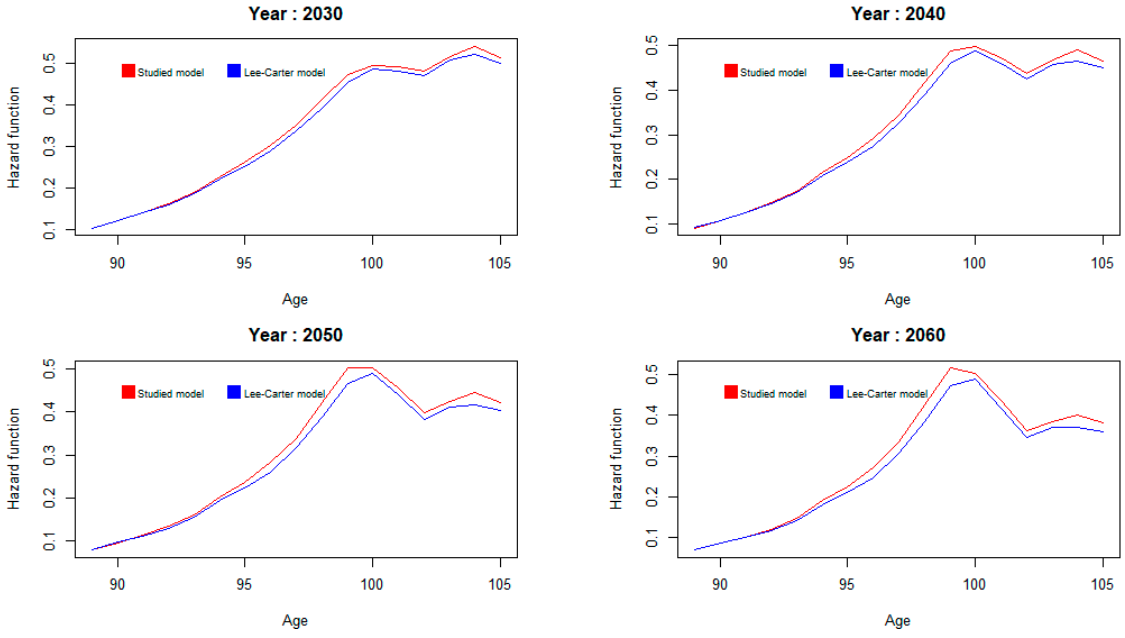

Figure 4. Mortality rates by age from 90 to 105 years.

The maximum relative deviation over the entire prospective range is 3.6% at age 80 for the year 2060.

We now compare the mortality forces of the two models over the entire prospective analysis period, for a few selected ages. This comparison is performed in Figure 5:

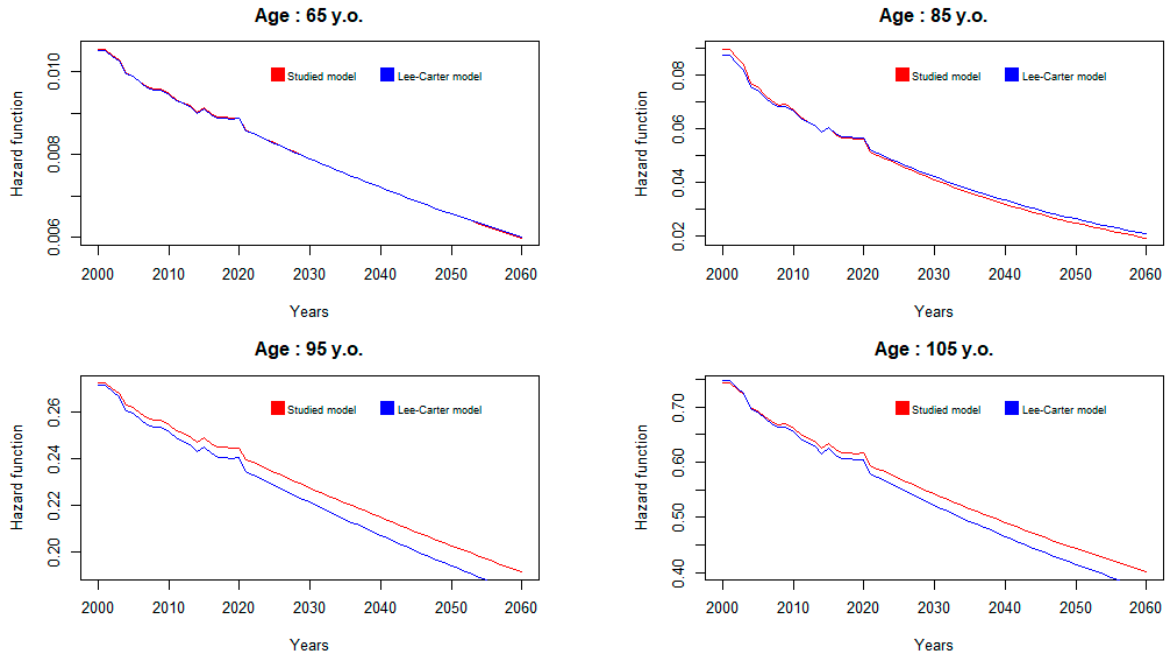

Figure 5. Mortality rates by year for selected ages.

Overall, the mortality model studied tends to predict higher mortality forces than the referenced Lee–Carter model at older ages, and the gap increases over time.

Before calculating prospective residual life expectancies, it is worth looking at the overall impact on mortality forces. To this end, we calculate the following ratio:

$$r(x,t) = \frac{\mu(x,t)}{\mu_{LC}(x,t)}$$

with $\mu_{LC}(x,t)$, the mortality force derived from the referenced Lee–Carter model and $\mu(x,t)$ model. This ratio is shown in the following figure (Figure 6):

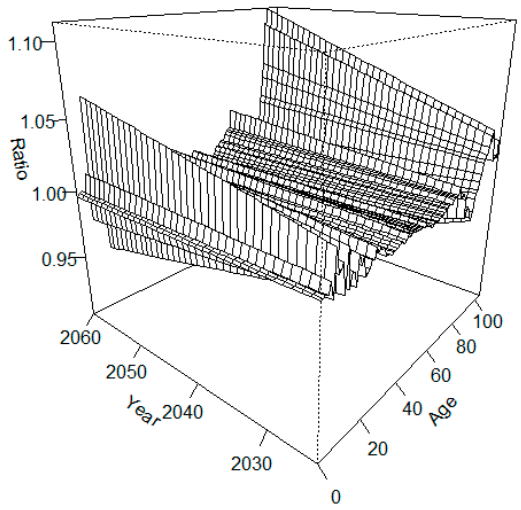

Figure 6. Mortality force ratio over the entire age range and prospective analysis period (2021 to 2060).

The average value of this ratio for all ages and years combined is 100%, which means that the model studied is equivalent to the Lee–Carter model. This reflects the assumption made that the expectation of the frailty factor is equal to one.

The impact of the introduction of shocks on adjustment is, therefore, negligible when assessed on a very global basis. However, the difference increases over time, leading the two models to diverge in the medium term and at older ages.

If we restrict ourselves to ages over 65, we obtain a weighted average equal to 99.8%.

In addition, the average mortality rate of the population, calculated on the basis of exposure to risk in 2020, evolves as represented on Figure 7:

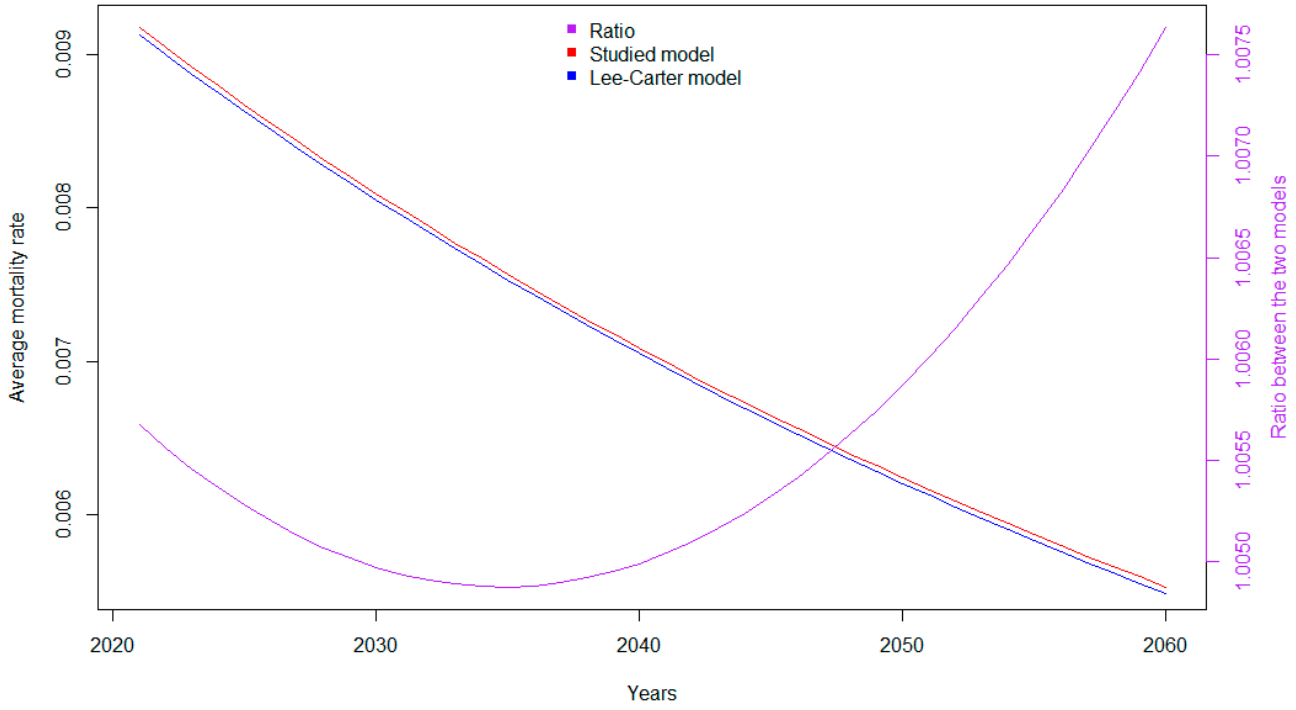

Figure 7. Average mortality rate per year, all ages combined, from 2021 to 2060.

It can be seen that the model studied is on average more pessimistic than the Lee–Carter model on mortality improvement in future mortality, with a projected average mortality rate that is slightly higher than that derived from the Lee–Carter model.

3.3. Estimating Prospective Residual Life Expectancies

It is then possible to look at the consequences of the mortality model studied on prospective residual life expectancies, first by variable age for a few fixed years, then by variable year for a few fixed ages.

As shown in Figure 8, it appears that the mortality model studied does not greatly change prospective residual life expectancies compared to the reference mortality model, except possibly at high ages:

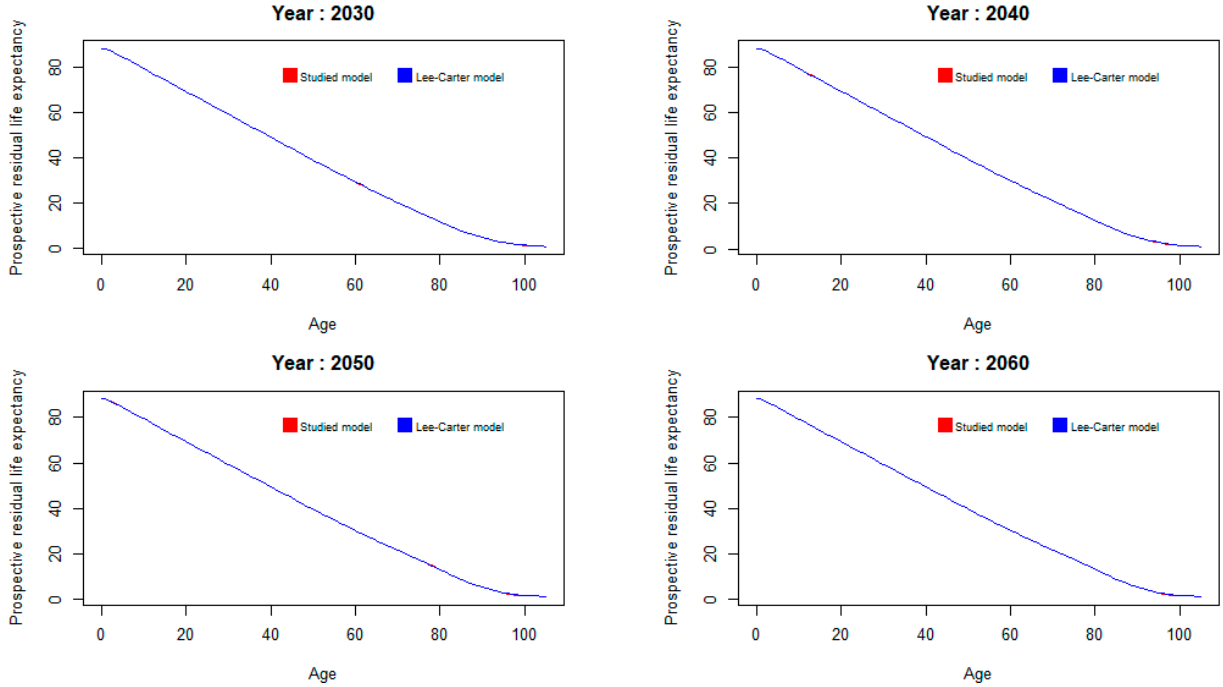

Figure 8. Trends in prospective residual life expectancy by age.

An enlargement of these graphs at older ages is shown below on Figure 9, with the algebraic difference between the two models for each year:

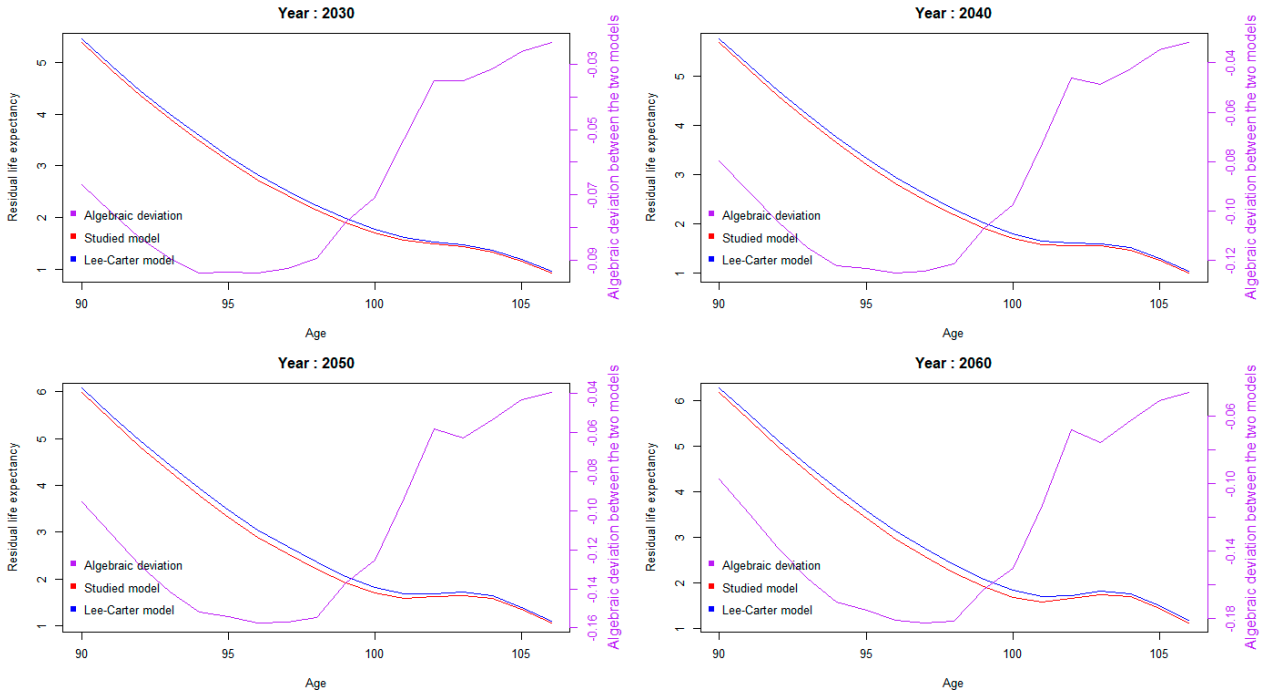

Figure 9. Change in prospective residual life expectancy from age 90 to 105.

The maximum absolute difference between the two models is found at age 96 for the year 2060, and it is worth 0.18, or around 65 days.

In this analysis, we return to the observation made in the previous section: he difference from the referenced Lee–Carter model is most marked for older ages, as shown on Figure 10.

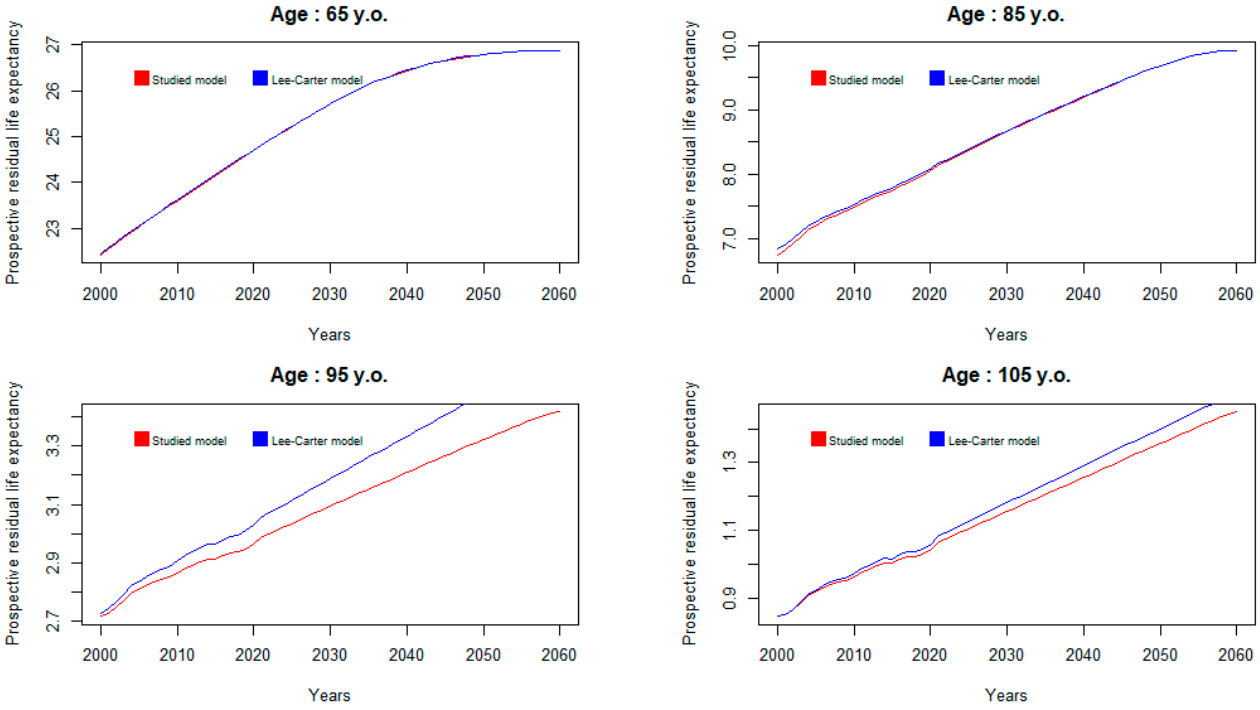

Figure 10. Prospective residual life expectancy by year.

Below on Figure 11 is an enlargement for age 96 with the algebraic difference between the two models:

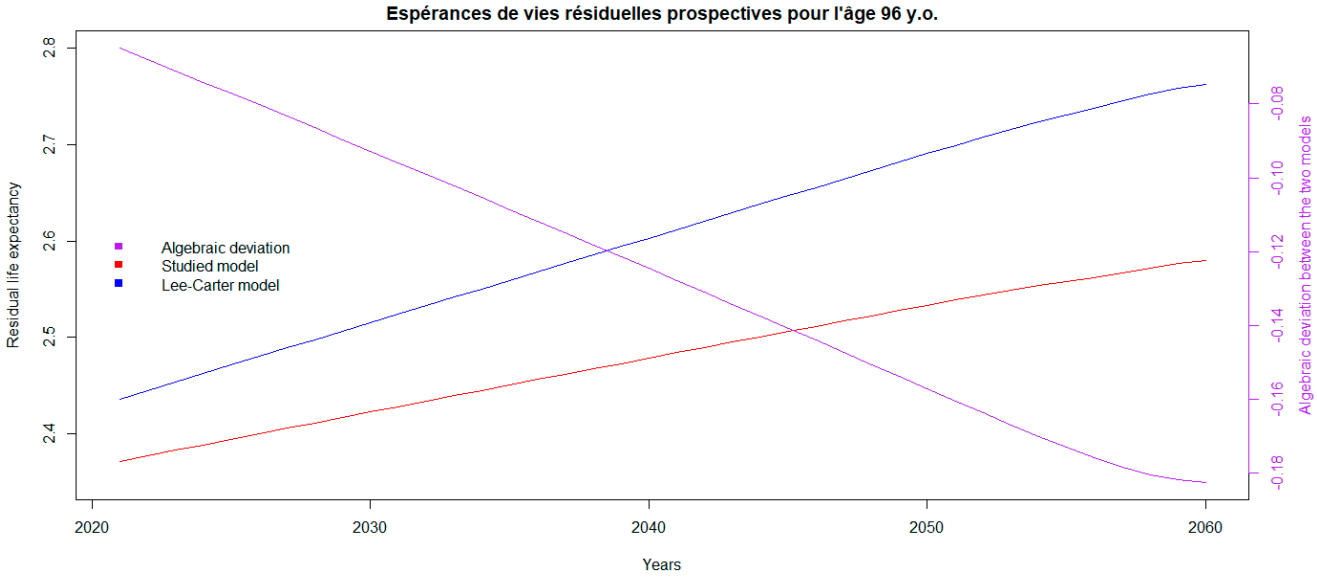

Figure 11. Trend in prospective residual life expectancy by year at age 96.

3.4. Sensitivity to Frailty Parameter

The volatility of frailty is estimated at 4.3%; however, over a longer period, this parameter can be higher. For example[4], from 1982 to 2022 it comes out at 5.5%.

With this level of volatility, we note that $P(Z_t \geq 1.09) \approx 5\%$. Noting that 9% is the excess mortality rate[5] for the year 2020, we can deduce that the probability of observing excess mortality at this level is of the order of 5%. Furthermore, $VaR_{99.5\%}(Z_t) \approx 1.15$, which corresponds to the mortality shock for the "mortality" risk module of the Solvency 2 delegated regulation. In other words,

- the severity of the COVID-19 pandemic remains below the Solvency 2 bicentennial event. It is associated with a 10-fold higher probability of occurrence.
- the calibration of frailty with a volatility of 5.5% is consistent with that of the Solvency 2 standard formula for mortality risk.

Based on the central table $\mu_0(x,t)$ adjusted above, the prospective residual life expectancies associated with a volatility coefficient of 5.5% are recalculated using

$$e(x,t) = \sum_{i\geq 0} \prod_{j=0}^{i} \left(\frac{\sigma^{-2}}{\sigma^{-2} + \mu_0(x+j, t+j)} \right)^{\sigma^{-2}},$$

which leads to the results presented on Figure 12:

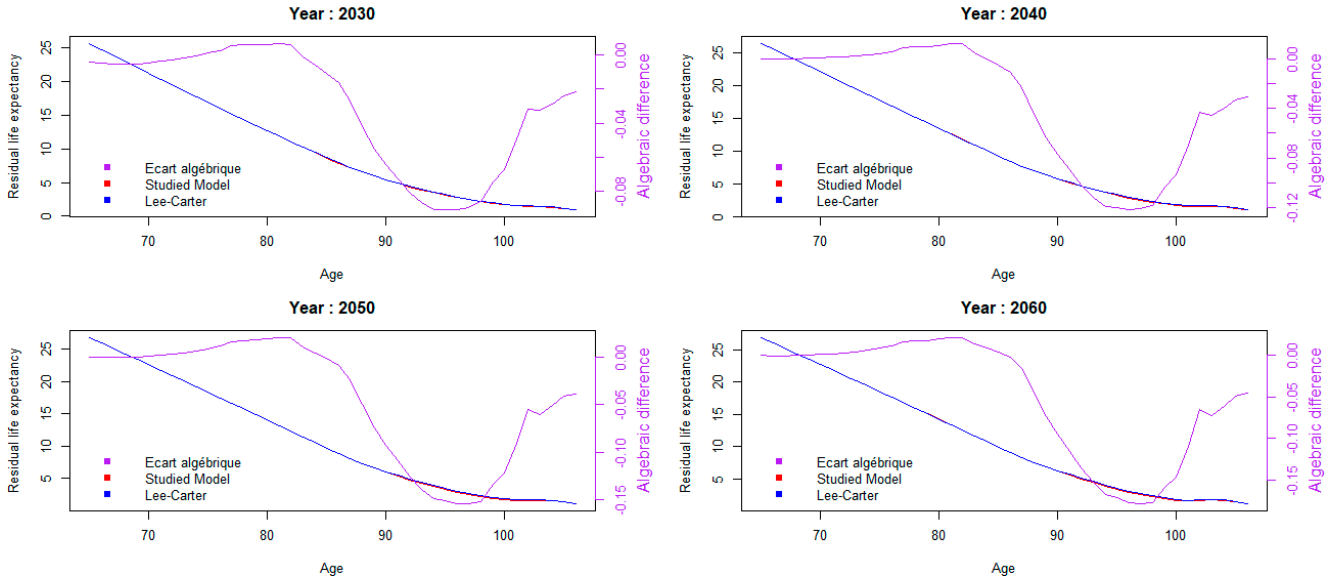

Figure 12. Evolution of prospective residual life expectancies from age 65 to 105 for selected years, with a new volatility coefficient.

There is no significant difference between the two models with this new volatility setting.

3.5. Consequences for the Capital Requirement of an Annuity Plan

The presence of the frailty factor, therefore, has no material impact on central tendency indicators (mortality forces, residual life expectancies, etc.).

However, the random nature of the mortality distribution in a given year has consequences for the assessment of the capital required to protect against adverse deviations in mortality. In the specific context of a life annuity plan, following a logic analogous to that of the Solvency 2 standard, we are led to consider the 99.5% quantile of the distribution of residual life expectancies induced by frailty as a proxy for the SCR[6]. For each age from 60 to 100, we obtain the following results (Figure 13) for the ratio between this quantile and the expectation, from a direct Monte-Carlo approach:

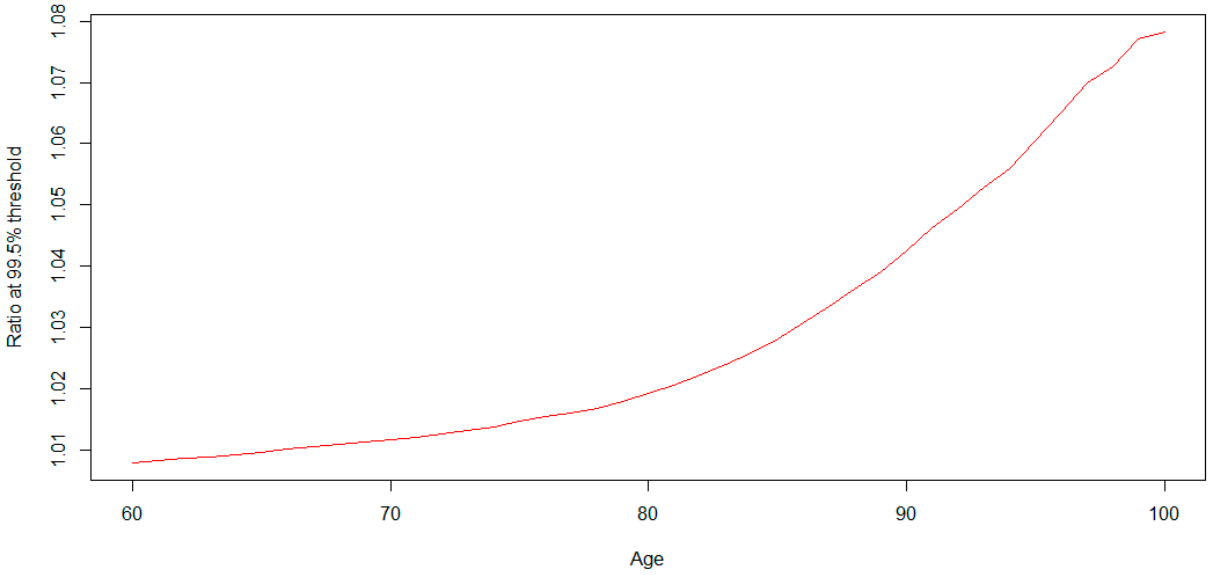

Figure 13. Ratio between 99.5% quantile and expectation (SCR).

Weighted by the age structure of the French population, the average ratio is around 101.3%.

For its part, the delegated regulation[7] imposes a 20% discount on death rates when calculating the SCR associated with longevity risk (cf. art. 138 of delegated regulation EU n°2015/35), which leads to a capital requirement equal to 10% of the expectation.

This means that the volatility observed in annual death rates explains around 12% of the longevity SCR.

4. Conclusions and Discussion

The use of a Gamma frailty model enables us to correctly account for the annual variations in mortality levels observed throughout France.

Incorporating these variations into the fitting of a forward-looking log-Poisson model poses no major difficulty, and a two-stage parameter estimation process enables us to use conventional likelihood maximisation algorithms.

The results obtained show that the impact of this additional volatility is negligible on the central tendency indicators. However, those results follow the assumption that the shocks are mean-centred. This document provides a more general structure to perform prospective analyses under situations of durable deterioration or amelioration of mortality (i.e., consider $E(Z_t) \neq 1$).

On the other hand, there is a material impact on the capital requirement associated with longevity risk, with just under 15% of this requirement being induced by the presence of this volatility. The remainder is associated with uncertainty about the trend in death rates.

Thus, while the main hazard associated with the construction of a prospective mortality table remains the uncertainty attached to the determination of the trend (see Juillard et al. (2008), Juillard and Planchet (2006) and Plat (2009) for detailed analyses on this point), considering these short-term fluctuations in mortality levels provides a better understanding of the determinants of longevity risk.

Finally, an important limitation of the proposed model is that the annual shock is applied with the same intensity to all ages. The determinants of shocks of this type over the last 40 years (typically heatwaves and/or flu epidemics or COVID-19) mainly concern older age groups (over 65). The model should, therefore, be refined on this point. However, this limitation needs to be put into perspective, as applications of this model mainly concern pension schemes, where participants are older.

Author Contributions: Conceptualization, F.P.; Methodology, G.G.d.L.P.; Software, G.G.d.L.P.; Data curation, G.G.d.L.P.; Writing—original draft, F.P.; supervision—F.P. All authors have read and agreed to the published version of the manuscript.

Funding: This research received no external funding.

Data Availability Statement: The data presented in this study are available on request from the corresponding author.

Conflicts of Interest: Authors Frédéric Planchet and Guillaume Gautier de la Plaine were employed by the company Prim'Act. The authors declare that the research was conducted in the absence of any commercial or financial relationships that could be construed as a potential conflict of interest. The company Prim'Act had no role in the design of the study; in the collection, analyses, or interpretation of data; in the writing of the manuscript, or in the decision to publish the results.

Appendix A

Table A1. Calibrated model coefficients (1/3).

Alpha								
Age	**Model Studied**	**LC Reference Model**	**Age**	**Model Studied**	**LC Reference Model**	**Age**	**Model Studied**	**LC Reference Model**
0	−5.6542	−5.6553	36	−7.0173	−7.0186	72	−4.0422	−4.0456
1	−7.3447	−7.3457	37	−6.9390	−6.9396	73	−3.9592	−3.9625
2	−8.2790	−8.2804	38	−6.8474	−6.8480	74	−3.8668	−3.8713
3	−8.6679	−8.6695	39	−6.7630	−6.7633	75	−3.7867	−3.7882
4	−8.9672	−8.9721	40	−6.6729	−6.6733	76	−3.6851	−3.6862
5	−9.0765	−9.0803	41	−6.5862	−6.5867	77	−3.5790	−3.5803
6	−9.1958	−9.2028	42	−6.4878	−6.4880	78	−3.4774	−3.4791
7	−9.2892	−9.2924	43	−6.3872	−6.3877	79	−3.3674	−3.3679
8	−9.4087	−9.4124	44	−6.2849	−6.2854	80	−3.2163	−3.2216
9	−9.3935	−9.4009	45	−6.1800	−6.1803	81	−3.0838	−3.0881
10	−9.4223	−9.4329	46	−6.0917	−6.0922	82	−2.9510	−2.9556
11	−9.3577	−9.3662	47	−5.9813	−5.9817	83	−2.8178	−2.8236
12	−9.2768	−9.2809	48	−5.8840	−5.8845	84	−2.6937	−2.7014
13	−9.1674	−9.1742	49	−5.7947	−5.7952	85	−2.5725	−2.5850
14	−8.9411	−8.9443	50	−5.7068	−5.7077	86	−2.4381	−2.4498
15	−8.6907	−8.6949	51	−5.6157	−5.6166	87	−2.3015	−2.3126
16	−8.4690	−8.4721	52	−5.5399	−5.5411	88	−2.1619	−2.1733
17	−8.2022	−8.2047	53	−5.4596	−5.4605	89	−2.0266	−2.0390
18	−7.9805	−7.9814	54	−5.3712	−5.3722	90	−1.8871	−1.9001
19	−7.7424	−7.7441	55	−5.2853	−5.2866	91	−1.7522	−1.7651
20	−7.6642	−7.6654	56	−5.2062	−5.2078	92	−1.6216	−1.6351
21	−7.6042	−7.6051	57	−5.1270	−5.1289	93	−1.4936	−1.5072
22	−7.5935	−7.5952	58	−5.0598	−5.0611	94	−1.3657	−1.3777
23	−7.5824	−7.5837	59	−4.9902	−4.9925	95	−1.2453	−1.2594
24	−7.5520	−7.5540	60	−4.9156	−4.9178	96	−1.1239	−1.1367
25	−7.5513	−7.5531	61	−4.8551	−4.8570	97	−1.0154	−1.0262
26	−7.5195	−7.5211	62	−4.7853	−4.7877	98	−0.9056	−0.9177
27	−7.4982	−7.4995	63	−4.7165	−4.7182	99	−0.8059	−0.8166
28	−7.4795	−7.4816	64	−4.6552	−4.6571	100	−0.7093	−0.7208
29	−7.4393	−7.4409	65	−4.5875	−4.5894	101	−0.6286	−0.6345
30	−7.3880	−7.3899	66	−4.5141	−4.5163	102	−0.5389	−0.5481
31	−7.3594	−7.3607	67	−4.4558	−4.4580	103	−0.4581	−0.4679
32	−7.3008	−7.3012	68	−4.3774	−4.3802	104	−0.4095	−0.4185
33	−7.2536	−7.2544	69	−4.2982	−4.3005	105	−0.4625	−0.4652
34	−7.1764	−7.1771	70	−4.2170	−4.2209			
35	−7.1106	−7.1110	71	−4.1381	−4.1415			

Table A2. Calibrated model coefficients (2/3).

Beta								
Age	**Model Studied**	**LC Reference Model**	**Age**	**Model Studied**	**LC Reference Model**	**Age**	**Model Studied**	**LC Reference Model**
0	0.0033	0.0033	36	0.0120	0.0120	72	0.0070	0.0071
1	0.0115	0.0115	37	0.0115	0.0115	73	0.0070	0.0071
2	0.0114	0.0114	38	0.0123	0.0123	74	0.0075	0.0077
3	0.0118	0.0117	39	0.0119	0.0118	75	0.0090	0.0091
4	0.0130	0.0131	40	0.0129	0.0129	76	0.0094	0.0094
5	0.0121	0.0118	41	0.0134	0.0135	77	0.0097	0.0097
6	0.0097	0.0102	42	0.0140	0.0140	78	0.0096	0.0097
7	0.0145	0.0146	43	0.0137	0.0137	79	0.0099	0.0098
8	0.0119	0.0121	44	0.0135	0.0136	80	0.0136	0.0129
9	0.0126	0.0127	45	0.0132	0.0133	81	0.0139	0.0134
10	0.0144	0.0138	46	0.0136	0.0137	82	0.0141	0.0137
11	0.0114	0.0118	47	0.0128	0.0127	83	0.0142	0.0137
12	0.0165	0.0162	48	0.0122	0.0122	84	0.0115	0.0107
13	0.0143	0.0142	49	0.0108	0.0108	85	0.0083	0.0073
14	0.0151	0.0151	50	0.0106	0.0106	86	0.0065	0.0057
15	0.0155	0.0151	51	0.0099	0.0099	87	0.0059	0.0054
16	0.0180	0.0182	52	0.0093	0.0093	88	0.0056	0.0052
17	0.0171	0.0171	53	0.0093	0.0093	89	0.0057	0.0054
18	0.0185	0.0187	54	0.0095	0.0094	90	0.0051	0.0049
19	0.0183	0.0180	55	0.0093	0.0092	91	0.0049	0.0048
20	0.0170	0.0169	56	0.0082	0.0080	92	0.0044	0.0046
21	0.0158	0.0158	57	0.0082	0.0081	93	0.0039	0.0041
22	0.0146	0.0146	58	0.0067	0.0066	94	0.0026	0.0030
23	0.0156	0.0156	59	0.0061	0.0059	95	0.0023	0.0027
24	0.0132	0.0134	60	0.0050	0.0049	96	0.0016	0.0024
25	0.0126	0.0127	61	0.0042	0.0041	97	0.0008	0.0014
26	0.0113	0.0115	62	0.0039	0.0038	98	−0.0005	0.0004
27	0.0111	0.0112	63	0.0040	0.0039	99	−0.0013	−0.0006
28	0.0107	0.0108	64	0.0042	0.0042	100	−0.0002	−0.0001
29	0.0088	0.0088	65	0.0038	0.0038	101	0.0018	0.0022
30	0.0103	0.0102	66	0.0046	0.0046	102	0.0044	0.0047
31	0.0111	0.0110	67	0.0050	0.0051	103	0.0046	0.0048
32	0.0107	0.0106	68	0.0047	0.0047	104	0.0046	0.0053
33	0.0105	0.0104	69	0.0059	0.0059	105	0.0046	0.0051
34	0.0106	0.0105	70	0.0055	0.0055			
35	0.0114	0.0113	71	0.0063	0.0064			

Table A3. Calibrated model coefficients (3/3).

Kappa					
Age	**Model Studied**	**LC Reference Model**	**Age**	**Model Studied**	**LC Reference Model**
2000	24.4565	24.4761	2030	−43.8008	−43.8043
2001	24.4627	24.5265	2031	−45.9908	−45.9945
2002	21.2073	21.2070	2032	−48.1809	−48.1847
2003	18.4710	18.4083	2033	−50.3709	−50.3750
2004	10.9651	10.9513	2034	−52.5610	−52.5652
2005	9.4399	9.4231	2035	−54.7510	−54.7554
2006	6.0386	6.0366	2036	−56.9410	−56.9456
2007	3.1599	3.1578	2037	−59.1311	−59.1358
2008	1.4649	1.4631	2038	−61.3211	−61.3260
2009	1.6981	1.6984	2039	−63.5112	−63.5163

Table A3. *Cont.*

Kappa					
Age	**Model Studied**	**LC Reference Model**	**Age**	**Model Studied**	**LC Reference Model**
2010	−1.1863	−1.1865	2040	−65.7012	−65.7065
2011	−4.7123	−4.7140	2041	−67.8912	−67.8967
2012	−6.6593	−6.6691	2042	−70.0813	−70.0869
2013	−8.5651	−8.5639	2043	−72.2713	−72.2771
2014	−12.6304	−12.6243	2044	−74.4614	−74.4673
2015	−9.8526	−9.8338	2045	−76.6514	−76.6575
2016	−13.5803	−13.5743	2046	−78.8414	−78.8478
2017	−15.8335	−15.8386	2047	−81.0315	−81.0380
2018	−15.6887	−15.6650	2048	−83.2215	−83.2282
2019	−16.4993	−16.4493	2049	−85.4116	−85.4184
2020	−16.1564	−16.2296	2050	−87.6016	−87.6086
2021	−24.0904	−24.0924	2051	−89.7916	−89.7988
2022	−26.2805	−26.2826	2052	−91.9817	−91.9891
2023	−28.4705	−28.4728	2053	−94.1717	−94.1793
2024	−30.6606	−30.6630	2054	−96.3618	−96.3695
2025	−32.8506	−32.8532	2055	−98.5518	−98.5597
2026	−35.0406	−35.0435	2056	−100.7418	−100.7499
2027	−37.2307	−37.2337	2057	−102.9319	−102.9401
2028	−39.4207	−39.4239	2058	−105.1219	−105.1304
2029	−41.6108	−41.6141	2059	−107.3120	−107.3206
			2060	−109.5020	−109.5108

Notes

1 It should be remembered that Lee and Carter's initial model is not a probabilistic model, and simply proposes a parsimonious decomposition of interactions between age and year in the structure of mortality rates across a country.

2 https://cran.r-project.org/web/packages/Rsolnp/index.html (accessed on 31 December 2023).

3 https://cran.r-project.org/web/packages/demography/index.html (accessed on 31 December 2023).

4 https://www.ressources-actuarielles.net/C1256F13006585B2/0/39B54166464089AFC12572B0003D88C2/$FILE/20230921_FP.pdf?OpenElement (accessed on 31 December 2023).

5 https://actudactuaires.typepad.com/laboratoire/2021/03/mortalit%C3%A9-en-france-en-2020-suite.html (accessed on 31 December 2023).

6 The SCR is the minimum capital required to control the probability of ruin at one year in the sense of the economic balance sheet at the level of 0.5%.

7 EU Delegated Regulation n°2015/35: https://eur-lex.europa.eu/legal-content/FR/TXT/?uri=CELEX:32015R0035 (accessed on 31 December 2023).

References

Agalva, Élisabeth, and Nathalie Blanpain. 2021. *Projections de Population 2021–2070*. Insee Résultats. Paris: INSEE.

Barbi, Elisabetta. 1999. Eterogeneità Della Popolazione e Sopravvivenza Umana: Prospettive Metodologiche ed Applicazioni alle Generazioni Italiane 1870–1895. Ph.D. thesis, Dipartimento Statistico, Università degli Studi di Firenze, Florence, Italy; 91p.

Barbi, Elisabetta, Graciella Casellic, and Jacques Vallin. 2003. Hétérogénéité des générations et âge extrême de la vie. *Population* 58: 45–68. [CrossRef]

Bongaarts, John. 2004. Long-range trends in adults mortality: Models and projection methods. *Demography* 42: 23–49. [CrossRef] [PubMed]

Brouhns, Natacha, Michael Denuit, and Jeroen K. Vermunt. 2002. A Poisson log-bilinear regression approach to the construction of projected lifetables. *Insurance, Mathematic and Economics* 31: 373–93. [CrossRef]

Carannante, Maria, Valeria D'Amato, Steven Haberma, and Massimilliano Menzietti. 2023. Frailty-based Lee–Carter family of stochastic mortality models. *Quality and Quantity*. [CrossRef]

Currie, Ian, Maria Durban, and Paul Eilers. 2003. Using P-splines to extrapolate two-dimensional Poisson data. Paper presented at the 18th International Workshop on Statistical Modelling, Leuven, Belgium, July 7–11.

Debonneuil, Edouard. 2015. Parametric age-dependent mortality model, for applications to retirement portfolios. In *Actuarial Thesis*. Lyon: ISFA.

Ghalanos, Alexios, and Stefan Theussl. 2015. Rsolnp: General Non-Linear Optimization. Available online: https://cran.r-project.org/package=Rsolnp (accessed on 31 December 2023).

Guette, Vivien. 2010. La prise en compte des catastrophes dans la modélisation de la mortalité. In *Actuary Thesis*. Lyon: ISFA.

Guilbaud, Corentin. 2018. Nouveaux modèles d'analyse et de projection de la mortalité, application a la population française. In *Mémoire d'Actuaire*. Paris: Dauphine.

Hyndman, Rob. 2023. Demography: Forecasting Mortality, Fertility, Migration and Population Data. Available online: https://cran.r-project.org/package=demography/index.html (accessed on 31 December 2023).

Juillard, Marc, and Frederic Planchet. 2006. Mesure de l'incertitude tendancielle sur la mortalité—Application à un régime de rentes. *Assurances et Gestion des Risques* 75: 357–74.

Juillard, Marc, Frédéric Planchet, and Pierre E. Thérond. 2008. Perturbations extrêmes sur la dérive de mortalité anticipée. *Assurances et Gestion des Risques* 76: 1–11.

Lee, Ronald D., and Lawrence R. Carter. 1992. Modeling and forecasting us mortality. *Journal of the American Statistical Association* 87: 659–71.

Planchet, Frédéric, and Pierre E. Thérond. 2011. *Modélisation Statistique des Phénomènes de Durée—Applications Actuarielles*. Paris: Economica.

Plat, Richard. 2009. On stochastic mortality modelling. *Insurance: Mathematics and Economics* 45: 393–404.

Robben, Jens, and Katrien Antonio. 2023. Catastrophe risk in a stochastic multi-population mortality model. *arXiv* arXiv:2306.15271.

Thatcher, A. R. 1999. The Long-term Pattern of Adult Mortality and the Highest Attained Age. *Journal of the Royal Statistical Society* 162: 5–43. [CrossRef] [PubMed]

Vaupel, James W., Kenneth Manton, and Eric Stallard. 1979. The impact of heterogeneity in individual frailty on the dynamics of mortality. *Demography* 16: 439–54. [CrossRef] [PubMed]

Ye, Yinyu. 1987. Interior Algorithms for Linear, Quadratic, and Linearly Constrained Non-Linear Programming. Ph.D. thesis, Department of EES Stanford University, Stanford, CA, USA.